2017 IEEE/RSJ International Conference on Intelligent Robots and Systems (IROS)
September 24–28, 2017, Vancouver, BC, Canada

NREL-Exo: a 4-DoFs Wearable Hip Exoskeleton for Walking and Balance Assistance in Locomotion*

Ting Zhang, *Member*, Minh Tran, and He (Helen) Huang, *Senior Member, IEEE*

Abstract—In this paper, we presented a high-power, self-balancing, passively and software-controlled active compliant, and wearable hip exoskeleton to provide walking and balance assistance. The device features powered hip abduction/adduction (HAA) and hip flexion/extension (HFE) modules to provide assistance in both sagittal and frontal planes. Each module's actuation unit employs a Series Elastic Actuator (SEA) to achieve passive compliance. The hip exoskeleton can work in two basic operation modes: human-in-charge and robot-in-charge. Both modes are integrated into the low-level controller based on the admittance control, making transitions smooth and stable. A new balance controller based on the "extrapolated center of mass" (XCoM) concept is presented for real-time control hip abduction/adduction to keep the center of mass (CoM) within the support polygon. The exoskeleton controller is designed to encourage participation in walking instead of overriding users' intrinsic behavior to achieve effective assistance and training. Our preliminary experiments on a healthy subject using the hip exoskeleton demonstrated the potential effectiveness of the device and controller in assisting locomotion.

I. Introduction

Individuals with neurological disorders suffer from decreased muscle activity and consequently insufficient hip torque during locomotion. This also often leads to decreased self-balancing capacities, which leaves these individuals vulnerable to unexpected falls. These setbacks can be mitigated with lower limb exoskeletons, which are considered a major step forward in assistive technology as well as robotics and rehabilitation engineering in general [1, 2]. Researchers and engineers, seeking to use the device to provide active assistance and reduce the users' walking effort, have brought about very promising results. Future exoskeletons are expected to help patients with physical disabilities effectively restore their normal walking ability and improve their quality of life.

Recently, lower-limb exoskeletons have begun to emerge, such as Mina [3], WPAL [4], including several hip exoskeletons [5, 6]. Emerging commercially available exoskeletons, such as ReWalk [7], Ekso [8], and Indego [9], have been primarily developed for restoration of mobility in paraplegic individuals. Most combat the balance issue with external devices such as crutches, but this solution increases the user's dependency and discourages motor learning [10]. Moreover, the user's arms won't be available for other tasks (e.g. holding objects, communicating nonverbally, etc). Li et al. designed a balance stabilizer mechanism, which can be used to enhance the stability of current available assistive exoskeleton [11]. However, it's also have limited mobility due to their large system size and weight. During walking, adapting step width is crucial for lateral stability as the lateral weight shift has been shown to precede the initiation of a step [12]. All of these lower-limb exoskeletons only have powered hip flexion/extension (HFE); the lacks of powered hip abduction/adduction (HAA) limits the capability of maintaining lateral stability and shift the lateral weight. The extrapolated center of mass (XCoM) is the vertical projection of the center of mass (CoM) in the direction of its velocity [13]. The XCoM concept has been successfully applied in analyzing human balance control [14]. Wang et al. developed an exoskeleton with powered HAA that incorporates the XCoM concept to adapt the step-width to counteract disturbances during gait [15, 16].

An important feature of the lower-limb exoskeletons balance control, which separates them from biped robots, is the participation of wearers in the balance control and decision making process [17]. This presents additional difficulties, as wearers inadvertently modulate their own muscle torques when the human-exoskeleton coupled system is losing balance under perturbation [18]. The exoskeleton should not override wearers' behaviors to provide assistance, but rather encourage their participation and avoid slacking. To fulfill this, the exoskeletons need to have capability to operate in two different modes: human-in-charge and robot-in-charge. In the human-in-charge mode, the exoskeleton should be able to follow the wearer's motion with transparency, and interaction force should be minimized during operation. In the robot-in-charge mode, the exoskeleton should be able to provide assistive loads to wearer as needed [19]. Existing exoskeleton controllers for the human–robot interaction do not provide much flexibility for collaboration tasks, and most require that the exoskeleton leads or follows the wearer after a real-time assessment of user performance [20]. To achieve compliant assistance, the exoskeleton controller should be able to provide a smooth transition between a robot-in-charge mode and a human-in-charge mode. Hard switching between these two control modes may result in an overall discontinuous control input, which can lead to compromises in device stability and even the safety and comfort of wearers [20].

The goal of this research is to develop a high-power, self-balancing, passively and software-controlled active compliant, and wearable hip exoskeleton for walking and balance assistance. The hip exoskeleton assists with hip flexion and extension, as well as hip abduction and adduction. The actuation unit employs a modular, compact and high torque-weight-ratio series elastic actuator (SEA), it will

*This work was supported in part by the NSF #1406750.

The authors are with the NCSU/UNC Joint Department of Biomedical Engineering, North Carolina State University, Raleigh, NC 27695 USA (e-mail:zhangt.hit@gmail.com).

endowing of passively compliant between the exoskeleton and the wearer interface. Important emphases and contributions of this paper are the following.

1) Development of a SEA-driven hip exoskeleton with powered HAA and HFE to maintain balance in both sagittal and frontal planes;

2) The assistant controller's effectiveness in easing the effort of the subjects during walking;

3) The lower-level controller based on admittance control provides a unified formulation for both the robot-in-charge mode, where the exoskeleton plays a dominant role to follow desired impedance, and the human-in-charge mode, in which the wearer is more active in guiding the movement of exoskeleton;

4) We incorporate the XCoM concept to assistive weight shift and adapt the step-width to counteract disturbances during walking.

II. NREL-EXO DESIGN

The purpose of developing NREL-EXO is to provide sufficient stable walking assistance in human locomotion. In order to perform walking tasks effectively, the structure of the exoskeleton is designed to be kinematically similar to the anatomy of the human hip and thigh.

A. Mechanical Design

The NREL-Exo is developed to assist patients who have muscular weakness but retain voluntary lower limb motor control with walking and remaining balance. To improve the synergy between the device and users, the joints and supporting structures are designed to be kinematically similar to the anatomy of the human hip and thigh. Our exoskeleton (shown in Fig. 1) is equipped with powered HFE as well as HAA joints on both limbs. These four single-axis revolute joints are securely connected to the wearer with two orthopedic braces and a back plate. All joints are highly modular, allowing actuation and/or sensing units to be easily installed or removed to fit the needs of different projects and applications. The device weighs 9.2 kg without the power source, which is fairly light compared to other rehabilitation exoskeletons, and includes adjustable sliding mechanisms. This allows users of different body sizes to quickly and comfortably adjust themselves to the exoskeleton.

The target maximal walking speed is 0.8m/s. This hip exoskeleton is supposed to be able to accommodate the anatomical measures of 90% of the adult population, which dictates the wearer height and hip width. The hip actuator should designed to provide a continue torque of 40Nm, maximum torque of 80Nm and maximum joint velocity of 150 deg/s based on the human hip angle and torque profiles form the Winter dataset. It can be assistance 50% of the human torque required during ground-level walking at a natural cadence of 105 steps/min and a user weight of 80 kg [2]. Each SEA module is driven by a rotating flat brushless DC motor (EC 90 flat, Maxon Motor, Sachseln, Switzerland) The motor has a continuous torque rating of 0.44 Nm, and is equipped with an incremental encoder (4095ppr, MILE, Maxon Motor, Sachseln, Switzerland). A harmonic gearbox (csd-25-100-2A-GR-BB, Harmonic Drive, Limburg, Germany) with a transmission ratio 100:1 is connected to the motor, resulting in nominal torque and velocity profiles of about 40 Nm and 150 deg/s. The peak torque is limited to 80 Nm to avoid overheating. The SEA was designed to have an angular series stiffness of 2 Nm/deg for ± 15 deg, and allows 30 Nm bidirectional torque loading. To minimize the torsion spring's dimensions and weight, the spring use monolithic disc shape. When the torque exceeds the torsion spring's peak torque, the internal hard stop will work to keep from being damaged. Each SEA module including kinematic and kinetic sensors weighs approximately 1.5 kg, 0.6 kg of which is from the motor.

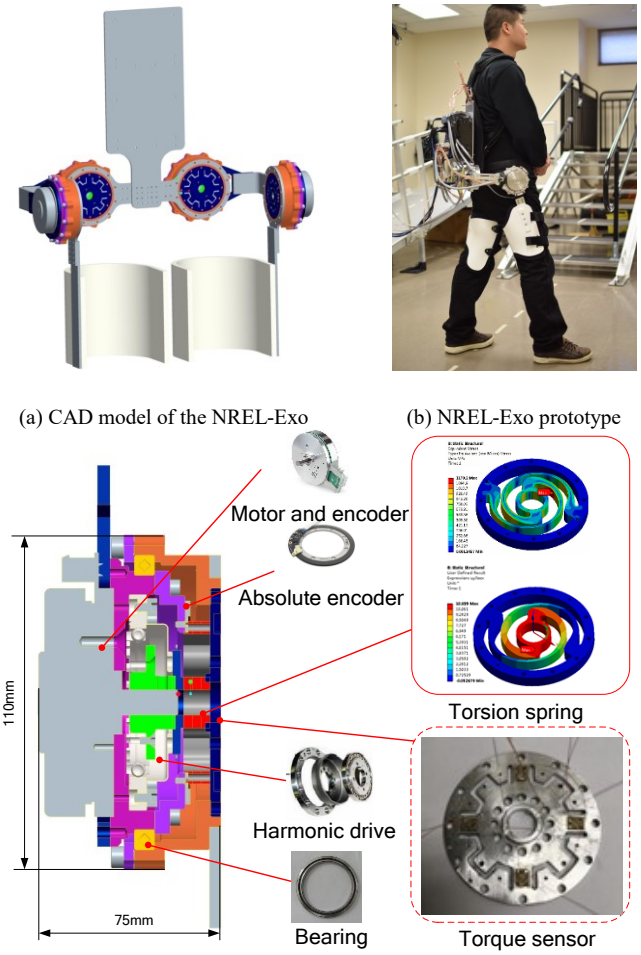

(a) CAD model of the NREL-Exo (b) NREL-Exo prototype

(c) Main modules of SEA

Fig. 1 Overview of the NREL-Exo

B. Control System

(1) Hardware of the control system

The control system is also modular design. Each joint is equipped with one 150 W commercial brushless motor driver (Copley Accelnet digital drive) to drive the motor and to provide feedback of the encoder and motor current data to the high-level control system. Each joint also uses a mini DSP chip to acquire data from the joint position and torque sensors. The high-level control system runs on a laptop. A CAN bus connects all elements of the hip exoskeleton, including both the high-level control system and the low-level control system. The lower-level control loop is updated at 2 kHz, with an inner current loop that is updated at 10 kHz, and the

control parameters are updated by the high-level controller at 100 Hz. The electrical system is powered by a 24 V benchtop DC power supply.

(2) High-level control

The exoskeleton controller must perform two main tasks: assistive walking and maintaining walking stability. Accordingly, the hip exoskeleton's control strategy can be subdivided into strategies for locomotion and balance control.

The scheme of control system is shown in Fig. 2. As implemented in the controller, a finite-state machine governs the walking behavior of the hip exoskeleton. During normal assistive walking, the hip exoskeleton is controlled by a high-level control scheme based on a finite-state-machine and a low-level control scheme based on admittance control. If any loss of stability is detected, the exoskeleton will immediately add a new control input to prevent the wearer from losing stability.

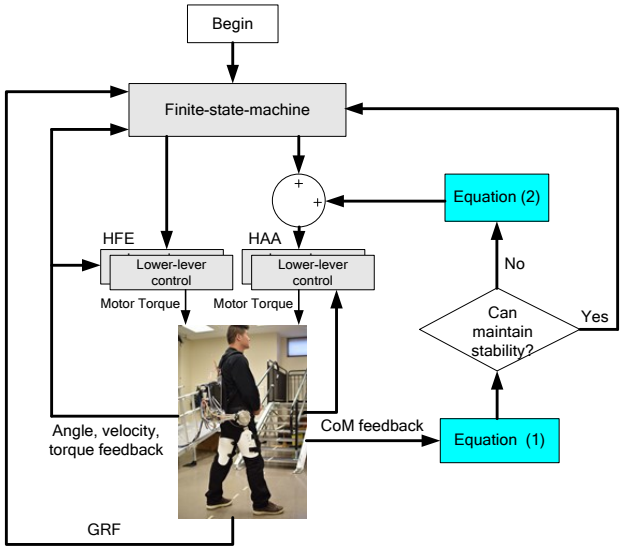

Fig. 2 Scheme of control system

Five gait-phase states are defined for assisted walking: left-leg early swing (flexion), left-leg late swing (extension), double support, right-leg early swing (flexion), and right-leg late swing (extension). Each state consists of parameters describing the impedance of the four hip joints, including the joint stiffness (K), damping (D) and equilibrium angle (θ_0), as well as transition criteria. During operation, the states are concatenated to produce seamless locomotion behavior. An admittance-based controller was chosen to cooperatively render the joint impedance with the integrated series compliance within the SEA mechanism.

We define a ratio to detect the disturbance:

$$r_{lateral} = \frac{y_{CoM}}{y_{LADP}} \tag{1}$$

where $r_{lateral}$ is the weight shift ratios in the frontal planes, respectively; y_{CoM} and y_{LADP} are the CoM position and step width, respectively, in the frontal plane is shown in Fig. 3. When the $r_{lateral}$ threaten the thresholds, the $\Delta\theta_d^{HAA}$ add to the finite state machine. The HAA adjustment angle is

$$\Delta\theta_d^{HAA} = \arcsin\left(\frac{\Delta \mathrm{XCoM}_y}{L} + sin\varphi\right) - \varphi \tag{2}$$

At each sample, $\Delta\theta_d^{HAA}$ can be computed and added to the nominal angle θ_d^{HAA}. The value of φ can be calculated from the HAA angles.

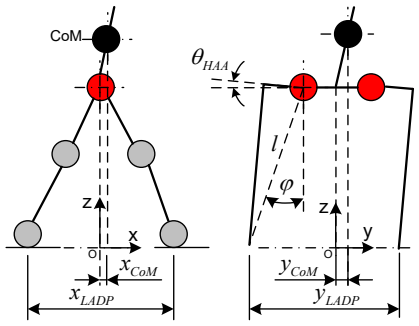

Fig. 3 Sketch of the estimation of the CoM position in the sagittal plane and in the frontal plane.

The XCoM position in the lateral plane is defined as

$$\mathrm{XCoM}_y = CoMy + \frac{v_{CoMy}}{\omega_0} \tag{3}$$

where $CoMy$ and v_{CoMy} are the lateral CoM position and velocity, respectively, and ω_0 is the eigenfrequency of the pendulum$\omega_0 = \sqrt{g/l}$, where l is the length of the pendulum and g is the acceleration due to gravity.

$$\begin{aligned} \Delta\mathrm{XCoM}_y &= \Delta CoMy + \frac{\Delta v_{CoMy}}{\omega_0} \\ &= CoMy - y_{CoM}^{bs} + \frac{v_{CoMz} - v_{CoMz}^{bs}}{\omega_0} \end{aligned} \tag{4}$$

where y_{CoM}^{bs} and v_{CoMz}^{bs} are the nominal values of the XCoM position and velocity during normal walking without perturbations and Δv_{CoMy} is the acceleration of $CoMy$.

(3) Lower-level control

The main difficulty in using an exoskeleton to increase the assistance of leg movements is that the exoskeleton's mechanism adds extra impedance to the legs. Given the current state of robotic technology, the implementation of a robotic lower-limb exoskeleton that is capable of biological levels of the joint torque and velocity will likely introduce nonnegligible mass, rotational inertia, and possibly joint friction [11]. The lower-level has the following input terms:

$$\tau_m = u_c + u_f + u_a \tag{5}$$

where u_c is a torque to compensate for the effect of the human leg motion, u_f is a torque to compensate for the effect of the friction, and u_a is a torque to the exoskeleton effort assistance.

A model-based feedback friction compensation scheme [21] is used. The following exponential friction model is chosen as the friction model:

$$\tau_f = \left(\alpha_0 + \alpha_1 e^{-(\dot{\theta}/v_s)^2}\right)\mathrm{sgn}(\dot{\theta}) + \alpha_2\dot{\theta} \tag{6}$$

where α_0 is the coefficient of Coulomb friction, α_1 is the coefficient of Stribeck friction, v_s is the characteristic velocity of the Stribeck friction, and α_2 is the coefficient of

viscous damping. The friction coefficients α_0, α_1, α_2 and v_s are identified using experiments.

The physical model of a SEA is

$$m\ddot{\theta}_m = \tau_m - k_s(\theta_m - \theta) - \tau_f \quad (7)$$

where m is the mass of the motor, θ_m is the motor angle, τ_m is the motor torque, θ is the joint angle, k_s is the stiffness of the SEA, and τ_f is the friction torque.

The SEA can be described as a function of τ

$$\ddot{\tau} = \frac{k_s}{m}\tau_m - \frac{k_s}{m}\tau - \frac{\alpha_2}{m}\dot{\tau} - k_s\ddot{\theta} - \frac{\alpha_2 k_s}{m}\dot{\theta} - \frac{k_s}{m}(\alpha_0 \mathrm{sgn}(\dot{\theta}) + \alpha_1 e^{-(\dot{\theta}/v_s)^2}\mathrm{sgn}(\dot{\theta})) \quad (8)$$

In (8), the human leg motion is reflected in the term $k_s\ddot{\theta} - \frac{\alpha_2 k_s}{m}\dot{\theta}$, and the friction torque is involved in the term $\frac{k_s}{m}(\alpha_0 \mathrm{sgn}(\dot{\theta}) + \alpha_1 e^{-(\dot{\theta}/v_s)^2}\mathrm{sgn}(\dot{\theta}))$.

Substituting (5) to (8) yields

$$\ddot{\tau} = \frac{k_s}{m}(u_c + u_f + u_a) - \frac{k_s}{m}\tau - \frac{\alpha_2}{m}\dot{\tau} - k_s\ddot{\theta} - \frac{\alpha_2 k_s}{m}\dot{\theta} - \frac{k_s}{m}(\alpha_0 \mathrm{sgn}(\dot{\theta}) + \alpha_1 e^{-(\dot{\theta}/v_s)^2}\mathrm{sgn}(\dot{\theta})) \quad (9)$$

u_c is designed to make the closed-loop system of the exoskeleton that interacts with the human leg have zero torque,

$$\frac{k_s}{m}u_c - k_s\ddot{\theta} - \frac{\alpha_2 k_s}{m}\dot{\theta} = 0 \quad (10)$$

u_f is designed to make the friction force completely compensated,

$$\frac{k_s}{m}u_f - \frac{k_s}{m}\left(\alpha_0 \mathrm{sgn}(\dot{\theta}) + \alpha_1 e^{-(\dot{\theta}/v_s)^2}\mathrm{sgn}(\dot{\theta})\right) = 0 \quad (11)$$

τ_c is designed as

$$u_c = \frac{m}{k_s}(k_s\ddot{\theta} + \frac{\alpha_2 k_s}{m}\dot{\theta}) \quad (12)$$

Thus, the friction compensation term is

$$u_f = \frac{m}{k_s}\left(\alpha_0 \mathrm{sgn}(\dot{\theta}) + \alpha_1 e^{-(\dot{\theta}/v_s)^2}\mathrm{sgn}(\dot{\theta})\right) \quad (13)$$

To establish a more compliant operation, we developed an algorithm that considered the interaction torque between the subject and the exoskeleton to produce an adaptive reference for the gait assistance. The adjusted reference trajectory θ_{adj} is given by (14), where s is the Laplace operator.

$$\begin{cases} \theta_{adj} = \theta_{ref} + \theta_{int} \\ \theta_{int} = \frac{1 - K/k_s}{K + D\dot{\theta}}\tau \end{cases} \quad (14)$$

θ_{ref} is a vector that contains the recorded angles based on the subject's gait, and θ_{int} is the angle that results from the interaction torque τ between the exoskeleton and the subject's limb. θ_{int} changes proportionally with the interaction torque and is estimated using the virtual impedance parameters D and K. The u_a is the output torque of the trajectory-tracking controller. The concept of assistance as needed is implemented by varying the joint stiffness. The variation in stiffness can be determined based on the performance of the wearer and the level of assistance to be exerted by the hip exoskeleton:

$$\begin{cases} K_{T+1} = K_T + \Delta K \\ \Delta K = \frac{\theta_{ref} - \theta}{\varepsilon\tau} \end{cases} \quad (15)$$

where ε is a confidence factor in the interval [0,1], which is used to determine the stiffness to be applied at sample time T + 1.

III. Experimental Characterization

In order to evaluate the functionality of the high-level control system, a prototypical task of gait assistance was designed and tested on a healthy volunteer (male, 30 years old, 70 kg). Prior to subject testing, mechanical parameters of the SEA must be identified. The parameters of the static friction model are identified as follow: $\alpha_0 = 1.5$ Nm, $\alpha_1 = 2.6$ Nm, $v_s = 0.004$ rad/s, $\alpha_2 = 4.2$ Nm · s/rad. The stiffness of the spring of the SEA was $k_s = 800$ Nm/rad; the motor rotor inertia is $B = 0.55$ Kgm^2. The rotor inertia of SEA was M = 0.014 Kg · m^2. The subject experimental protocol has been approved by the IRB at the University of North Carolina at Chapel Hill, and all human subjects were consented before the experiment. The experiment platform is shown in Fig. 4.

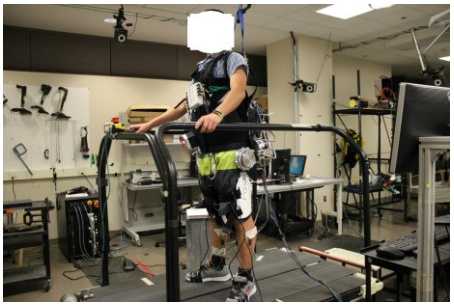

Fig.4 Experiment platform

A. Characterization of human-in-charge mode

For this experiment, the NREL-Exo was driven with the zero-torque control scheme. It was expected that the exoskeleton was totally transparent to the subject, which meant the interaction torque would be nearly nonexistent.

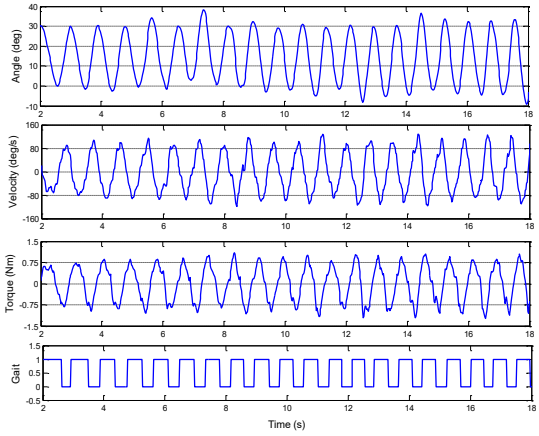

Fig. 5 Validation of the human-in–charge control of left leg. Gait phases: 0-stand phase, 1-swing phase

During operation, human-in-charge would be activated if the user's output torque matched that of the exoskeleton, or if the human response was totally different from the device and assistance needed to be disabled to achieve compliance.

This scheme could be achieved by setting the impedance parameters in eq. (15) to zero and eliminating the active assistance torque u_a in the controller. Experimental results shown in Fig. 5 verified this hypothesis. Throughout the trials, the interaction torque remained very close to zero with an absolute maximum value smaller than 1.1 Nm. At all velocities tested, the zero-impedance control was stable.

B. Characterization of walking assistance

In this test scenario, an admittance-based framework was used to calculate and generate the assistive torque. The needed torques provided by SEA modules were determined with every joint's impedance property, which consisted of a passive spring and a damper and was characterized by a fixed equilibrium position. Different sets of impedance properties were used at different periods during gait as shown in Table 1. Gait phases were determined with force sensors located at the subject's shoe insoles.

Table 1 IMPEDANCE PARAMETERS

Gait phase	Stiffness (Nm/deg)		Damping ($\mathrm{Nm/deg \cdot s^{-1}}$)		equilibrium angle (deg)	
	HFE	HAA	HFE	HAA	HFE	HAA
early swing	0.6	0.2	0.06	0.02	40	0
late swing	0.6	0.2	0.06	0.02	0	0
stance	0.2	0.2	0.02	0.02	-10	0

Every joint's angular position and velocity, motor current, and interaction torque data between exoskeleton and the subject's limb were collected for online control and post-testing data analysis. For kinematic and dynamic parameters, positive values corresponded to hip extension. The motor current turned to positive when the motor provides positive power and to negative when the motor provide negative power to the subject. Data collected in forty continuous gait cycles are averaged and presented as normalized plots (red lines) in Fig. 5.

During normal walking, assistance was only provided in the flexion-extension direction. As a result, each limb's lateral angles were naturally below 10 deg during stance and around 0 deg during swing, implying that equilibrium was reached as in Fig. 7(a). From Fig.7 (b), it can be seen that the trajectory of CoM was kept within the safe region in which stability can be maintained. Fig.7(c) demonstrates the exoskeleton's assistance to the subject throughout the gait cycle. The controller was expected to provide positive torque during extension, and negative torque during flexion. Looking at experimental results, it can be seen that the angle-torque relationship of both limbs closely followed this requirement. Also, the angle and torque plots were smooth with only a small jitter during stance. This indicates that a safe and compliant interaction was achieved and unwanted vibrations were suppressed with the adaptive control scheme.

To verify the assistant controller's effectiveness in easing the effort of the subjects during walking, sEMG signals from rectus femoris (hip flexor) and biceps femoris (hip extensor) muscles were collected and processed offline. Raw EMG signals were collected using a Delsys Bagnoli-8 system (Natick, MA, USA) with an amplification gain of 1000 at a sampling rate of 1000 Hz. The most notable result from Figs. 6 is a significant reduction in EMG activities of the agonist–antagonist muscle pair of the hip joint when the assistive function of the exoskeleton was used, which indicates that less effort is required from the subject.

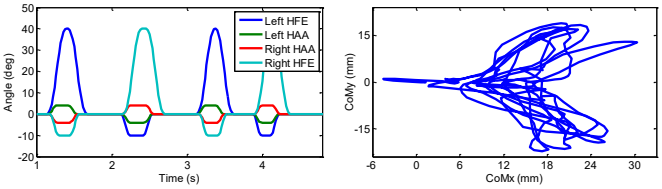

(a) Hip joints angle (b) Trajectory of CoM

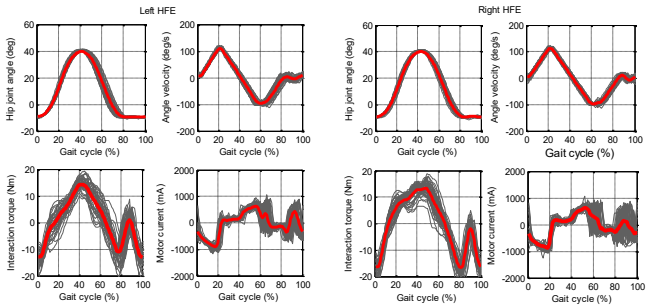

(c) Sensor feedback of HFE

Fig.6 The results of exoskeleton assistive normal walking

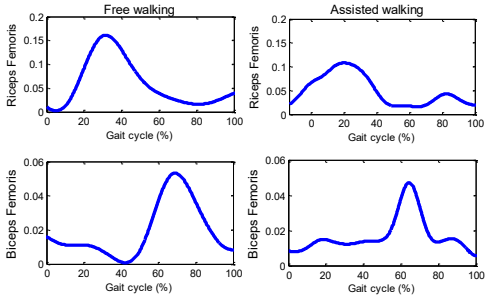

Fig. 7 Mean normalized sEMG activity of left leg for each tested condition in the gait cycle (%).

C. Characterization of balance assistance in locomotion

The aim of this experiment was to validate the balance controller. In this test, the subject wearing the exoskeleton was asked to walk straight over level ground. A safety harness worn by the subject was attached to an overhead suspension system moving along with the subject. The harness came into action only when the subject lost balance. On some steps, a slight push was manually applied to the subject's shoulder at the beginning of the swing phase. Two types of perturbations were applied (pushing from the stance side to the swing side and vice versa). Experimental results from a representative trial are shown in Fig. 8.

In this trial, perturbations were introduced at approximately 8.6 s and 10.8 s. For the perturbation applied at 8.6 s, the current gait phase was the left-leg swing, and the perturbation was from the swing side to the stance side. This resulted in both HAA joints attempting to shift the wearer's weight to his left leg to avoid further tilting to the right. For the perturbation applied at 10.8 s, the current gait phase was also the left-leg swing, but the direction of the perturbation was reversed. The results showed higher hip abduction levels

in both joints at the heel strike and a wider step width, as seen in Fig. 8 (f). After each perturbation, all angle changes returned to their values for normal walking. During the period after a perturbation, the torque profile deviated from the values observed during normal walking to accommodate the sudden perturbation. At approximately 6.1 s (red oval), the interaction torque at the left and right HAA joints were negative and positive, respectively. However, at 9 s (after perturbation I), the left HAA torque was positive, and the right HAA torque was negative. Although both instances occurred in the leg swing period, the assistive torques provided by the two HAA actuators reversed direction after the disturbance to produce angle profiles similar to those during normal walking to successfully assist in balance recovery.

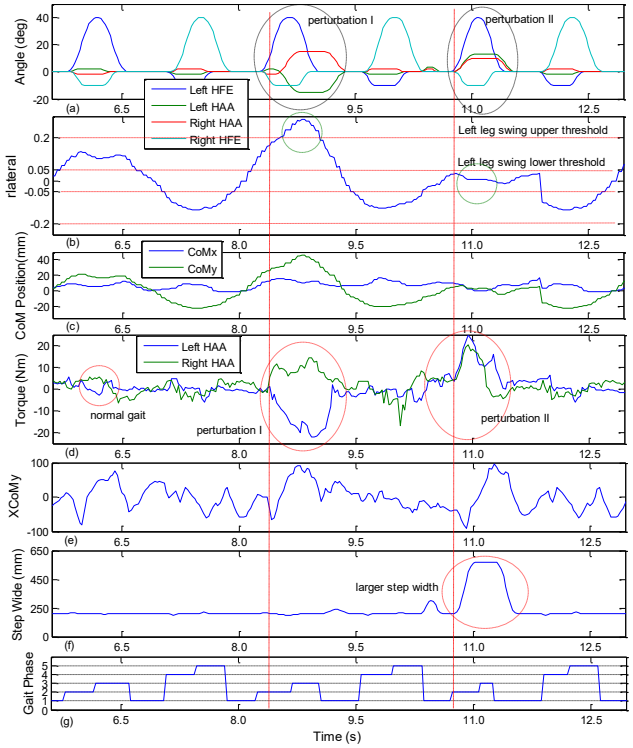

Fig. 8 Results for straight walking with step-width correction. (a) Joint angles. (b) Weight shift ratios in the lateral plane, $r_{lateral}$. (c) XCoMy. (d) CoM position. (e) Interact torque. (f) Step width. (g) Gait phase. Gait phases: 1- double support, 2- left-leg early swing (flexion), 3- left-leg late swing (extension), 4- right-leg early swing (flexion), 5- right-leg late swing (extension). The red vertical lines indicate the times of the perturbations.

IV. Conclusion

This paper describes a novel design and implementation of a hip exoskeleton with powered HFE and HAA joints to support walking and balance. Each actuation unit employs a modular and compact SEA with a high torque-to-weight ratio to make the device passively compliant. The hip exoskeleton can work with two basic operation modes: human-in-charge and robot-in-charge. Both modes are integrated into the low-level controller, making transitions smooth and stable. In the human-in-charge mode, the exoskeleton is able to follow the wearer's motion with minimal interaction force. In the robot-in-charge mode, the exoskeleton synergizes with the subject throughout the gait cycle to effective provide assistance and reduce walking effort. In the event of disturbances, the online step-width adjustment controller based on the XCoM concept maintains the gait stability of the coupled human-exoskeleton system.

References

[1] T. Yana, M. Cempinia, C. M. Oddoa, N. Vitielloa, "Review of Assistive Strategies in Powered Lower-Limb Orthoses and Exoskeletons", *Journal Robotics and Autonomous Systems*, Vol. 64, Issue C, pp. 120-136, 2015.

[2] Aaron J. Young and Daniel P. Ferris, "State-of-the-art and Future Directions for Lower Limb Robotic Exoskeletons", *IEEE Transactions on Neural Systems and Rehabilitation Engineering*, DOI 10.1109/TNSRE.2016.2521160, 2016.

[3] Anil K. Raj, Peter D. Neuhaus, Adrien M. Moucheboeuf, Jerryll H. Noorden, and David V. Lecoutre, "Mina: A Sensorimotor Robotic Orthosis for Mobility Assistance," *Journal of Robotics*, vol. 2011, Article ID 284352, 8 pages, 2011.

[4] Tanabe S, Hirano S, Saitoh E, "Wearable Power-Assist Locomotor (WPAL) for supporting upright walking in persons with paraplegia", *NeuroRehabilitation*, 33(1), pp.99-106, 2013.

[5] F. Giovacchini, F.Vannetti, M. Fantozzi, M. Cempini, M. Cortese, A. Parri, T. Yan, D. Lefeber, N. Vitiello, "A light-weight active orthosis for hip movement assistance", *Robotics and Autonomous Systems*, Vol. 73, pp. 123-134, 2015.

[6] SUITX. Available: http://www.suitx.com/phoenix.

[7] ARGO Medical Technology Ltd., http://rewalk.com/rewalk-personal-3/, 2016.

[8] Ekso Bionics, http://eksobionics.com/, 2016.

[9] S. A. Murray, K. H. Ha, C. Hartigan, and M.Goldfarb, An Assistive Control Approach for a Lower-Limb Exoskeleton to Facilitate Recovery of Walking Following Stroke, *IEEE Transactions on Neural Systems and Rehabilitation Engineering*, Vol. 23, No. 3, pp. 441-449, 2015.

[10] C. D. MacKinnon and D. A. Winter, "Control of whole body balance in the frontal plane during human walking," *J. Biomech.*, vol. 26, no. 6, pp. 633-644, 1993.

[11] L. Li, K. H. Hoon, A. Tow, P.H. Lim, and K. H. Low, "Design and Control of Robotic Exoskeleton with Balance Stabilizer Mechanism", 2015 IEEE/RSJ International Conference on Intelligent Robots and Systems (IROS) Congress Center Hamburg, Sept 28 - Oct 2, Hamburg, Germany, pp. 3817-3823, 2015.

[12] J. Pratt, et al., "Capture point: A step toward humanoid push recovery," in Humanoid Robots, 2006 6th IEEE-RAS, pp. 200-207, 2006.

[13] A. L. Hof et al., "The condition for dynamic stability," J. Biomech., vol. 38, no. 1, pp. 1–8, 2005.

[14] A. L. Hof, "The 'extrapolated center of mass' concept suggests a simple control of balance in walking," *Human Movement Sci*., vol. 27, no. 1, pp. 112–125, Feb. 2008.

[15] L. Wang, S. Wang, E. H. F. v. Asseldonk, H. v. d. Kooij, "Actively Controlled Lateral Gait Assistance in a Lower Limb Exoskeleton", 2013 IEEE/RSJ International Conference on Intelligent Robots and Systems (IROS) November 3-7, 2013. Tokyo, Japan, 965-970.

[16] S. Wang, L. Wang, C. Meijneke, E. v. Asseldonk, T. Hoellinger, et al "Design and Control of the MINDWALKER Exoskeleton", *IEEE Transactions on Neural Systems and Rehabilitation Engineering*, Vol. 23, No. 2, 277-286, 2015.

[17] B. Ugurlu, C. Doppmann, M. Hamaya, P. Forni, T. Teramae, T. Noda, and J. Morimoto, "Variable Ankle Stiffness Improves Balance Control: Experiments on a Bipedal Exoskeleton", *IEEE/ASME Transactions on Mechatronics*, Vol. 21, No. 1, pp. 79-87, 2016.

[18] D. Martelli, F. Vannetti, M. Cortese, P. Tropea, F. Giovacchini, S. Micera, V. Monaco, N. Vitiello, "The effects on biomechanics of walking and balance recovery in a novel pelvis exoskeleton during zero-torque control," *Robotica*, vol. 32(8):1317-1330, 2014.

[19] H. Yu, S. Huang, G. Chen, Y. Pan, and Z. Guo, Human-Robot Interaction Control of Rehabilitation Robots with Series Elastic Actuators, *IEEE Transactions on Robotics*, vol. 31, pp. 1089-1100, Oct. 2015.

[20] X. Li, Y. Pan, G. Chen and H. Yu, "Adaptive Human–Robot Interaction Control for Robots Driven by Series Elastic Actuators," *IEEE Transactions on Robotics*, vol. 33, no. 1, pp. 169-182, 2017.